Available online at www.sciencedirect.com
ScienceDirect
Journal of Nutritional Biochemistry 18 (2007) 587–596
Journal of Nutritional Biochemistry

Epigallocatechin-3-gallate suppresses NF-κB activation and phosphorylation of p38 MAPK and JNK in human astrocytoma U373MG cells

Su-Jin Kim[a,c], Hyun-Ja Jeong[a], Kang-Min Lee[b], Noh-Yil Myung[c], Nyeon-Hyoung An[c], Woong Mo Yang[d], Seong Kyu Park[d], Hye-Jung Lee[e], Seung-Heon Hong[c], Hyung-Min Kim[a], Jae-Young Um[a,e,*]

[a]*Department of Pharmacology, College of Oriental Medicine, Institute of Oriental Medicine, Kyung Hee University, 1 Hoegi-Dong, Dongdaemun-Gu, Seoul 130-701, Republic of Korea*
[b]*Division of Biological Sciences, College of Natural Science, Chounbuk National University, Jeonju, Jeonbuk 561-756, Republic of Korea*
[c]*College of Pharmacy, Wonkwang University, Iksan, Jeonbuk 570-749, Republic of Korea*
[d]*Department of Prescriptionology, College of Oriental Medicine, Kyung Hee University, 1 Hoegi-Dong, Dongdaemun-Gu, Seoul 130-701, Republic of Korea*
[e]*Acupuncture and Meridian Science Research Center, Kyung Hee University, 1 Seocheon-dong, Giheung-gu, Yongin-si, Gyeonggi-do 446-701, Republic of Korea*

Received 1 May 2006; received in revised form 10 November 2006; accepted 20 November 2006

Abstract

Epigallocatechin-3-gallate (EGCG) is the major polyphenol component of green tea and is primarily responsible for the green tea effect. EGCG possesses two triphenolic groups in its structure. These groups are reported to be important with respect to anticarcinogenic and antioxidant effects. However, the anti-inflammatory effect of EGCG on Alzheimer's disease (AD) is still not fully understood. In this study, we investigated the effects of EGCG in attenuating the inflammatory response induced by interleukin (IL)-1β+β-amyloid (25–35) fragment (Aβ) in human astrocytoma, U373MG cells. EGCG significantly inhibited the IL-1β+Aβ (25–35)-induced IL-6, IL-8, vascular endothelial growth factor (VEGF) and prostaglandin (PG)E_2 production at 24 h ($P<.01$). The maximal inhibition rate of IL-6, IL-8, VEGF and PGE_2 production by EGCG was approximately 54.40%, 56.01%, 69.06% and 47.03%, respectively. EGCG also attenuated the expression of cyclooxygenase-2 and activation of nuclear factor-κB induced by IL-1β+Aβ (25–35). We demonstrated that EGCG suppresses IL-1β+Aβ (25–35)-induced phosphorylation of the mitogen-activated protein kinase p38 and the c-Jun N-terminal kinase. In addition, EGCG induced the expression of mitogen-activated protein kinase phosphatase-1. These results provide new insight into the pharmacological actions of EGCG and its potential therapeutic application to various neurodegenerative diseases such as AD.

Keywords: Alzheimer's disease; Interleukin-6; Interleukin-8; Cyclooxygenase-2; Mitogen-activated protein kinase p38; c-Jun N-terminal kinase

1. Introduction

Alzheimer's disease (AD) is a degenerative disease of the brain, which causes dementia. AD is characterized by three main pathogenic factors: senile plaques, neurofibrillary tangles and inflammation [1]. The participation of the local inflammatory reaction has been confirmed especially by the results of studies dealing with activated microglia, reactive astrocytes, cytokines, reactive mediators of oxygen, and nitrogen (free radicals), all of which participate significantly in inflammatory processes [2]. These inflammatory markers are locally produced by brain cells and occur in close proximity of β-amyloid fragment (Aβ) deposits [3]. Aβ peptide induces the pro-inflammatory cytokine and chemokine secretion in rat astrocytes and human astrocytoma cells [4,5]. An inflammatory cytokine, interleukin (IL)-6, is overexpressed in AD brains, and an elevated production of IL-6 has been linked to early stages of Aβ deposition and

* Corresponding author. Department of Pharmacology, College of Oriental Medicine, Institute of Oriental Medicine, Kyung Hee University, 1 Hoegi-Dong, Dongdaemun-Gu, Seoul 130-701, Republic of Korea. Tel.: +82 2 961 9262; fax: +82 2 967 7707.
E-mail address: jyum@khu.ac.kr (J.-Y. Um).

0955-2863/$ – see front matter © 2007 Elsevier Inc. All rights reserved.
doi:10.1016/j.jnutbio.2006.11.001

plaque formation [6]. The chemokine IL-8 is a low-molecular-weight protein produced by a wide range of cells including microglia and astrocytes. Vascular endothelial growth factor (VEGF) plays a key role in physiological blood vessel formation and pathological neovascularization [7–9]. Expression of VEGF and its receptor in various organs including the brain is up-regulated in response to a hypoxic or hypoglycemic stress that presented in AD [10,11]. Prostaglandin (PG) E_2, a major PG in the brain of mammals, is the major lipid mediator. Reactive astrocytes that locate around plaques of AD brains increase the secretion of PGE_2 by evoked activity of cyclooxygenase (COX)-2. COX enzymes exist in a constitutive form, COX-1, and an inducible form, COX-2; the latter has been found to be elevated in the AD brain. Increased levels of COX-2 expression in astrocytes surrounding Aβ contribute to neurotoxicity and damage in the AD brain [12].

The mitogen-activated protein kinase (MAPK) signaling pathways regulate cellular process including gene expression, differentiation and cell death [13]. The most well-characterized members of the MAPK family include p38 MAPK, the extracellular-regulated kinase (ERK) p44 and the c-Jun N-terminal kinase (JNK). An increasing number of studies are demonstrating that activities of these kinases are changed in AD model [14]. The p38 MAPK pathway, a major proinflammatory signal transduction pathway, is hyperactive in the AD brain [15]. The p38 pathway was activated in the cortex and hippocampus of a patient with AD [16].

MAPK phosphatase (MKP)-1 is a critical negative regulator in response to inflammatory stimuli and is responsible for switching off the production of proinflammatory cytokines. The three MAP kinases are normally dephosphorylated by MKP-1 [17]. It was reported that inhibition of MKP-1 expression prolonged the cytokine production induced by p38 and JNK kinase phosphorylation [18].

Polyphenols of green tea, which comprise 30% of the dry weight of green tea leaves, include epigallocatechin-3-gallate (EGCG), epigallocatechin, epicatechin-3-gallate and epicatechin. Polyphenolic compounds in green tea have recently received considerable attention as preventive agents against hippocampal neuronal damage following transient global ischemia, cardiovascular disease and cancer [19–21]. EGCG is the most abundant of these catechins and is associated with many healthful benefits. Recently, several studies reported that EGCG regulates anti-inflammatory properties. For example, orally applied EGCG suppressed inflammation in vivo, inhibiting proliferation and TNF-α synthesis of T cells, and effectively protected against relapsing central nervous system (CNS) autoimmune disease [22]. In collagen-induced experimental arthritis, application of unpurified green tea extracts reduced anti-collagen Ig levels and the expression of the proinflammatory cytokines TNF-α and IFN-γ in arthritic joints [23]. Other research reported that EGCG up-regulates COX-2 expression and PGE_2 production in raw 264.7 macrophage cells [24], suggesting that EGCG may enhance inflammatory processes. In sum, the effects of EGCG on inflammatory response remain uncertain.

In order to elucidate the mechanism of EGCG underlying its apparent anti-inflammatory effect, we examined the effect of EGCG on expression of inflammatory genes, the NF-κB pathway in IL-1β+Aβ [25–35] fragment [Aβ (25–35)]-stimulated human astrocytoma, U373MG cells. In addition, we investigated the effects of EGCG on MAPK activation and MKP-1 expression.

2. Materials and methods

2.1. Reagents

Cell culture medium, RPMI 1640, ampicillin and streptomycin were purchased from Gibco BRL (Grand Island, NY, USA). Avidin peroxides, Aβ (25–35) fragment, 3-[4,5-dimethylthiazol-2-yl]-2,5-diphenyltetrazoliumbromide (MTT) and other reagents were obtained from Sigma (St. Louis, MO, USA). Anti-human IL-6 and IL-8, biotinylated anti-human IL-6 and IL-8, and recombinant human (rh) IL-6 and IL-8 were purchased from Pharmingen (San Diego, CA, USA). Anti-human VEGF antibody (Ab), biotinylated anti-human VEGF, rh VEGF and IL-1β were purchased from R&D Systems (Minneapolis, MN, USA). SB203580, SP600125 and EGCG were purchased from Calbiochem (San Diego, CA, USA). Antibodies for human COX-2, NF-κB, IκB-α, p38, pp38, JNK, pJNK were obtained from Santa Cruz Biotechnology (Santa Cruz, CA, USA).

2.2. Cell culture

Human astrocytoma cell line U373MG was obtained from the Korean Cell Line Bank. This cell is the common primary tumor in the brain and is typically angiogenic and characteristically exhibits endothelial cell hyperplasia. Cells were seeded into plates and maintained in RPMI 1640 medium (Gibco RBL) supplemented with 10% fetal bovine serum (FBS) and 1% penicillin (100 U/ml)/streptomycin (100 μg/ml) at 37°C under 5% CO_2 in air.

2.3. MTT assay

Cell viability was determined via an MTT assay. Briefly, 500 μl of cells suspension (3×10^5 cells) was cultured for 24 h after pretreatment with each concentration of EGCG. Fifty microliters of MTT solution (5 mg/ml) was added and the cells were incubated for 4 h at 37°C. After washing out the supernatant, the insoluble formazan product was dissolved in DMSO. The optical density of the 96-well culture plates was then measured using an enzyme-linked immunosorbent assay (ELISA) reader at 540 nm. The optical density of formazan formed in the untreated control cells was taken as 100% of viability.

2.4. Cytokine assay

IL-6, IL-8 and VEGF secretion was measured by a modified ELISA, as described previously [25]. The ELISA

was devised by coating 96-well plates of mouse monoclonal Ab with specificity for IL-6, IL-8 and VEGF. Before subsequent steps in the assay, the coated plates were washed with PBS containing 0.05% Tween 20. All reagents used in this assay were incubated for 2 h at 37°C. Recombinant IL-6, IL-8 and VEGF were diluted and used as a standard. Serial dilutions starting from 10 ng/ml were used to establish the standard curve. Assay plates were exposed sequentially to biotinylated mouse IL-6, IL-8 and VEGF avidin peroxidase, and ABTS substrate solution containing 30% H_2O_2. The plates were read at 405 nm.

2.5. PGE_2 production assay

The PGE_2 level was quantified using immunoassay kits according to the manufacturer's protocols (R&D Systems).

2.6. RT-PCR analysis

Total RNA was isolated from cells according to the manufacturer's specification using an easy-BLUE RNA extraction kit (iNtRON Biotech, Korea). Total RNA (2.5 μg) was heated at 65°C for 10 min and then chilled on ice. Each sample was reverse-transcribed to cDNA for 90 min at 37°C using a cDNA synthesis kit (Amersham Pharmacia, Minneapolis, USA). PCR was performed with the following primers for human (h) COX-2 (5′-TTC AAA TGA GAT TGT GGG AAA ATT GCT-3′; 5′-AGA TCA TCT CTG CCT GAG TAT CTT-3′), IL-8 (5′-CGA TGT CAG TGC ATA AAG ACA-3′; 5′-TGA ATT CTC AGC CCT CTT CAA AAA-3′), IL-6 (5′-GAT GGA TGC TTC CAA TCT GGA T-3′; 5′-AGT TCT CCA TAG AGA ACA ACA TA-3′), VEGF (5′-CGG GAT CCC GAT GAA CCT TCT GCT GTC TTG GGT-3′; 5′-CGG AAG CCC GTC ACC GCC TCG GCT TGT-3′), MKP-1 (5′-CGA TTA GTC CTC ATA AGG TA-3′; 5′-GCT GTG CAG CCA ACA GTC GA-3′). GAPDH (5′-CAA AAG GGT CAT CAT CTC TG-3′; 5′-CCT GCT TCA CCA CCT TCT TG-3′) were used to verify whether equal amounts of RNA were used for reverse transcription and PCR amplification from different experimental conditions. The annealing temperature was 60°C for IL-8, 50°C for IL-6, 57°C for VEGF, 55°C for COX-2, 57°C for MKP-1 and 60°C for GAPDH, respectively. Products were electrophoresed on a 1.5% agarose gel and visualized by staining with ethidium bromide. GAPDH mRNA was used as a control of mRNA loading.

2.7. Preparation of cytoplasmic and nuclear extract

Nuclear and cytoplasmic extracts were prepared as described previously [26]. Briefly, after cell activation, cells were washed with ice-cold phosphate-buffered saline (PBS) and resuspended in 60 μl of buffer A (10 mM Hepes/KOH, 2 mM $MgCl_2$, 0.1 mM EDTA, 10 mM KCl, 1 mM DTT and 0.5 mM PMSF, pH 7.9). The cells were allowed to swell on ice for 15 min, lysed gently with 2.5 μl of 10% Nonide P (NP)-40 and centrifuged at 2000×*g* for 10 min at 4°C. The supernatant was collected and used as cytoplasmic extract. The nuclei pellet was resuspended in 40 μl of buffer B (50 mM HEPES/KOH, 50 mM KCl, 300 mM NaCl, 0.1 mM EDTA, 10% glycerol, 1 mM DTT and 0.5 mM PMSF, pH 7.9), left on ice for 20 min and inverted. The nuclear debris was then spun down at 15,000×*g* for 15 min. The supernatant (nuclear extract) was collected, frozen in liquid nitrogen and stored at −70°C until ready for analysis.

2.8. Western blot analysis

For analysis of the phosphorylated or total protein level of indicated proteins in the text, stimulated cells were rinsed twice with ice-cold PBS and then lysed in ice-cold lysis buffer (PBS containing 0.1% SDS, 1% triton and 1% deoxycholate). Cell lysates were centrifuged at 15,000×*g* for 5 min at 4°C; the supernatant was then mixed with an equal volume of 2× SDS sample buffer, boiled for 5 min and then separated through a 10% denaturing protein gel. After electrophoresis, the protein was transferred to nylon membranes by electrophoretic transfer. The membranes were blocked in 5% skim milk for 2 h, rinsed and incubated overnight at 4°C with primary antibodies. After three washes in PBST/0.1% Tween 20, the membranes were incubated for 1 h with HRP-conjugated secondary antibodies. After three washes in PBST/0.1% Tween 20, the protein bands were visualized by an enhanced chemiluminescence assay (Amersham Pharmacia Biotech, New Jersey, USA) following the manufacturer's instructions.

2.9. Transcription factor enzyme-linked immunoassay (TF-EIA)

To investigate the effect of EGCG on NF-κB DNA binding activity, we performed a NF-κB TF-EIA assay. This assay has the advantage of being 10 times more sensitive than electrophoretic mobility shift assay and allows greater flexibility in the experimental step. Avidin peroxidase was coated a 96-well ELISA plate. The coated plate was washed with PBST and then blocked with 3% skim milk solution. It was then incubated with 1 μg/ml of 5′-biotinylated 21 single-strand DNA oligonucleotide sequence for 1 h at room temperature. This sequence contains the previously described NF-κB binding motif. The sequences used here were 5′-AGT TGA GGG GAC

Table 1
Effect of EGCG on cell viability in human astrocytoma U373MG cells

	Cell viability (%)
Blank	100.0±1.3
IL-1β+Aβ	97.92±3.5*
0.2 μM EGCG+IL-1β+Aβ	101.01±4.2
2 μM EGCG+IL-1β+Aβ	98.42±3.7
20 μM EGCG+IL-1β+Aβ	106.01±4.1**
200 μM EGCG+IL-1β+Aβ	74.650±4.5**

Cell viability was evaluated by MTT colorimetric assay after 24 h of incubation after stimulation of IL-1β (10 ng/ml) plus Aβ (25–35) (30 μM), in the absence or presence of EGCG (0.2–200 μM). Data represent the mean±S.E.M. of three independent experiments.

* $P<.05$, significantly different from the unstimulated cells.

** $P<.05$, significantly different from the IL-1β+Aβ-stimulated cells.

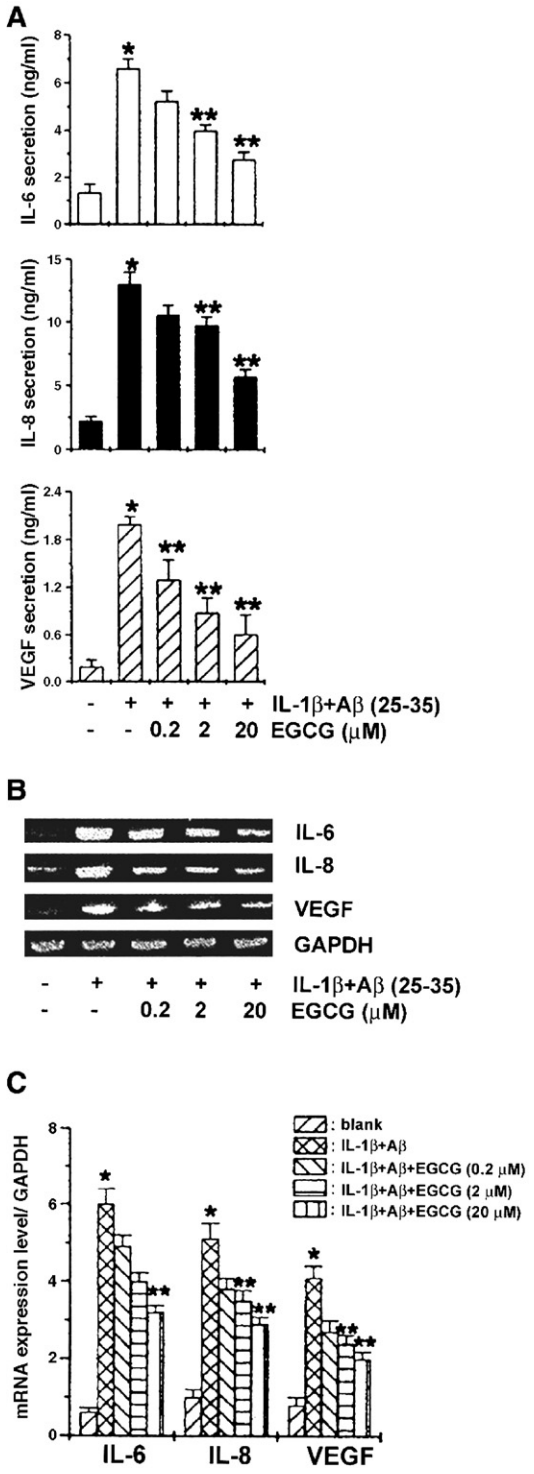

Fig. 1. Effect of EGCG on cytokine production and expression in U373MG cells at various concentrations. (A) U373MG cells (3×10^5) were pretreated with EGCG (0.2–20 μM) for 2 h and then treated with IL-1β (10 ng/ml) plus Aβ (25–35) (30 μM) for 24 h. The amount of IL-6, IL-8 and VEGF production was measured using the ELISA method. (B) Cells (5×10^6) pretreated with EGCG (0.2–20 μM) for 2 h and then treated with IL-1β (10 ng/ml) plus Aβ (30 μM) for 12 h. The level of IL-6, IL-8 and VEGF expression was measured using RT-PCR. (C) The relative intensity of cytokine mRNA level was quantitated by densitometry. Data represent the mean±S.E.M. of three independent experiments. *$P<.05$, significantly different from the unstimulated cells. **$P<.05$, significantly different from the IL-1β plus Aβ (25–35)-stimulated cells.

TTT CCC AGG-3′. DNA binding reaction was carried out in tissue protein containing 10 mM HEPES (pH 7.9), 50 mM NaCl, 5% glycerol, 1 mM EDTA and 1 mM DTT, for 1 h at room temperature and then washed. NF-κB antibodies were then added. After three washes in PBST/0.1% Tween 20, the corresponding alkaline phosphatase (AP)-coupled secondary antibody was added. AP activity was then detected by the addition of *p*-nitrophenyl phosphate solution (Sigma). After a 10-min incubation period, the reaction was arrested by the addition of 0.5 M H_2SO_4. Color intensity was detected at 405 nm using an ELISA reader. AP activity was normalized to control values (unstimulated cells). Protein was determined using a bicinchoninic acid (Sigma).

2.10. Immunocytochemistry and confocal microscopy

Cells were fixed with 3% paraformaldehyde and incubated with 5% BSA in PBS for 60 min. The preparation was subsequently incubated for 1 h at room temperature with MKP-1 Ab diluted in 0.1% bovine serum albumin (1:500). Next, the preparation was washed three times with PBS and then exposed to the secondary Ab (fluorescein isothiocyanate-conjugated anti-rabbit IgG at 1:200 and 0.1% BSA/PBS) for 60 min. The fluorescent image was viewed with an Olympus confocal microscope (New Hyde Park, NY, USA).

2.11. Statistical analysis

The experiments shown are a summary of the data from at least three experiments and are presented as the mean ± SEM. Statistical evaluation of the results was performed by an independent *t*-test.

3. Results

3.1. Effect of EGCG on production and expression of IL-6, IL-8 and VEGF

First, we examined the effect of EGCG on the viability of cells using MTT assay. Cells were treated with various concentrations of EGCG (0.2–200 μM) and then stimulated with IL-1β+Aβ for 24 h. In the cells treated with IL-1β+Aβ, cell viability decreased to 97.92±3.5% compared with the control value (100.0±1.3%). EGCG (0.2–20 μM) did not affect cell viability in each condition but high concentration of EGCG (200 μM) had toxicity on human astrocytoma, U373MG cells (Table 1). To investigate the effect of EGCG on inflammatory response induced by IL-1β+Aβ (25–35), the concentration of 0.2–20 μM EGCG was used in this study.

The influence of EGCG at various concentrations on production of IL-6, IL-8 and VEGF was tested after 24 h of activation with IL-1β+Aβ (25–35). As shown in Fig. 1A, IL-6, IL-8 and VEGF production were increased with treatment of IL-1β+Aβ (25–35). These increases were significantly inhibited by pretreatment of EGCG in a

dose-dependent manner. The maximal inhibition rate of IL-6, IL-8 and VEGF production by EGCG (20 μM) was approximately 57.80%, 56.01% and 69.01%, respectively.

The influence of EGCG at various concentrations on mRNA expression of IL-6, IL-8 and VEGF was tested after 12 h of activation with IL-1β+Aβ (25–35). As shown in Fig. 1B, mRNA expression level of IL-6, IL-8 and VEGF was increased with treatment of IL-1β+Aβ (25–35). These increases were significantly inhibited by pretreatment of EGCG in a dose-dependent manner. The maximal inhibition rate of IL-6, IL-8 and VEGF mRNA expression level by EGCG (20 μM) was about 46.60%, 42.01% and 48.01%, respectively. The relative intensity of the mRNA expression level was quantitated by densitometry (Fig. 1C).

3.2. Effect of EGCG on PGE2 production and COX-2 expression

In order to investigate the effect of EGCG on PGE_2 production, cells were pretreated with EGCG (0.2–20 μM) and then treated with IL-1β+Aβ (25–35) for 24 h. As shown in Fig. 2A, PGE_2 production in response to IL-1β+Aβ (25–35) was significantly inhibited by pretreatment with EGCG (0.2–20 μM) in a dose-dependent manner. The maximal inhibition rate of PGE_2 production by EGCG (20 μM) was 47.03±2.4% ($P<.05$).

To determine the effect of EGCG on induced COX-2 expression human astrocytoma, U373MG cells, RT-PCR and Western blotting were performed. As indicated by the data shown in Fig. 2B, treatment with IL-1β+Aβ (25–35) caused a significant increase in the COX-2 mRNA level. Pretreatment of EGCG (0.2–20 μM) resulted in the inhibition of COX-2 mRNA expression in a dose-dependent manner. According to the data shown in Fig. 2C, treatment with IL-1β+Aβ (25–35) caused a significant increase in the COX-2 protein level. Pretreatment of EGCG (0.2–20 μM) resulted in the inhibition of COX-2 protein expression in a dose-dependent manner.

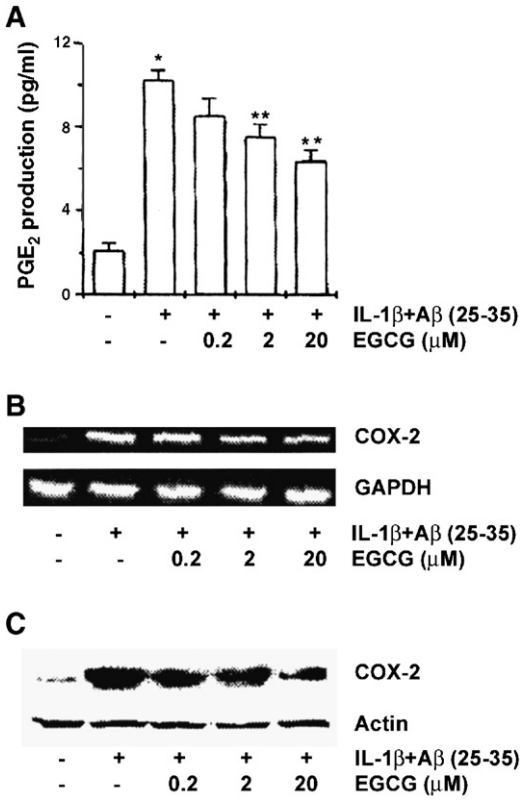

Fig. 2. Effect of EGCG on PGE_2 production and COX-2 expression in IL-1β plus Aβ (25–35)-stimulated U373MG cells. (A) U373MG cells (3×10^5) were pretreated with EGCG (0.2–20 μM) for 2 h and then treated with IL-1β (10 ng/ml) plus Aβ (25–35) (30 μM) for 24 h. The amount of PGE_2 production was measured using immunoassay kits. (B) U373MG cells (5×10^6 cells/ml) were pretreated with EGCG (0.2–20 μM) for 2 h and then treated with IL-1β (10 ng/ml) plus Aβ (25–35) (30 μM) for 12 h. COX-2 mRNA level was assayed by RT-PCR. (C) Cells (5×10^6 cells/ml) were pretreated with EGCG (0.2–20 μM) for 2 h and then treated with IL-1β (10 ng/ml) plus Aβ (25–35) (30 μM) for 24 h. The protein extracts were assayed by Western blot analysis for COX-2. *$P<.05$, significantly different from the unstimulated cells. **$P<.05$, significantly different from the IL-1β plus Aβ-stimulated cells.

3.3. Effect of EGCG on NF-κB activation

Because suppression of NF-κB activation has been linked with anti-inflammation, we postulated that EGCG mediates its effects at least partly through suppression of NF-κB activation. Since NF-κB activation requires nuclear translocation of the *Rel*A/p65 subunit of NF-κB, we examined the effect of EGCG on the nuclear pool of *Rel*A/p65 protein by Western blot analysis in human astrocytoma, U373MG cells. As shown in Fig. 3A, IL-1β+Aβ (25–35) treatment considerably increased the nuclear *Rel*A/p65 protein level, indicating nuclear translocation of *Rel*A/p65. Pretreatment of EGCG (20 μM) inhibited the IL-1β+Aβ (25–35)-stimulated increase of the nuclear *Rel*A/p65 levels in U373MG. In addition, IL-1β+Aβ (25–35) treatment effectively induced IκB-α degradation in human astrocytoma, U373MG cells. We also showed that EGCG (20 μM) significantly inhibited IL-1β+Aβ (25–35)-induced IκB-α degradation (Fig. 3B). These results suggested that EGCG blocks the nuclear translocation of *Rel*A/p65 from the cytoplasm.

To investigate the effect of EGCG on NF-κB DNA binding activity as well as attenuation of NF-κB expression in nuclear, we performed a NF-κB TF-EIA assay. As shown in Fig. 3C, treatment of IL-1β+Aβ (25–35) increased DNA-binding activity for NF-κB. However, enhanced binding activity was significantly decreased by EGCG pretreatment.

3.4. Effect of EGCG on MAPK signaling pathways

It was reported that enhancement of cytokine occurs through induction and activation of p38 and/or JNK pathway in human astrocytoma cells. It was also shown that inhibitors of ERK and PI3 did not regulate the cytokine production [27]. To test whether p38 and JNK regulate the cytokine production induced by IL-1β+Aβ (25–35), we

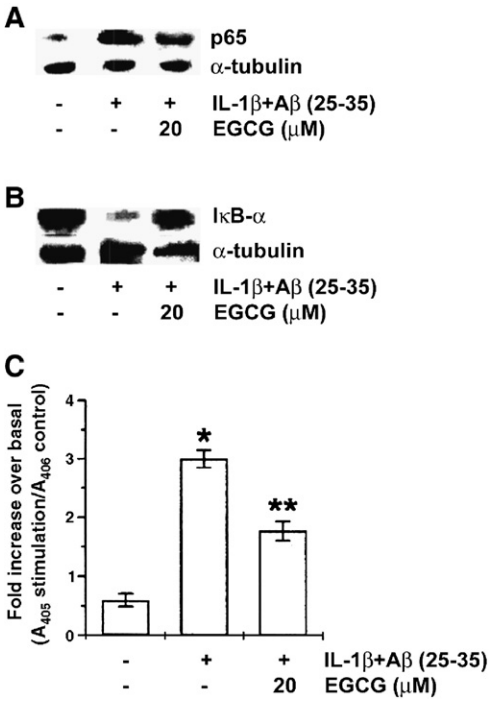

Fig. 3. Effect of EGCG on NF-κB activation and IκB-α degradation in IL-1β plus Aβ (25–35)-stimulated U373MG cells. (A) Cells (6×10^6) were preincubated for 2 h with EGCG (20 μM) and then treated with IL-1β (10 ng/ml) plus Aβ (25–35) (30 μM) for 2 h. The nuclear extracts were determined for *Rel*A/p65 by Western blot analysis. (B) The cytosolic extracts were determined for IκB-α by Western blot analysis. (C) Cells (6×10^6) were preincubated for 2 h with EGCG (20 μM) and then treated with IL-1β (10 ng/ml) plus Aβ (25–35) (30 μM) for 2 h. The nuclear extracts were determined for NF-κB DNA binding activity by TF-EIA. Each datum represents the mean±S.E.M. of three independent experiments. *$P<.05$, significantly different from the unstimulated cells. **$P<.05$, significantly different from the IL-1β plus Aβ-stimulated cells.

pretreated p38 inhibitor (SB203580) and JNK inhibitor (SP600125) for 1 h before IL-1β+Aβ (25–35) stimulation. Pretreatments with MAPK inhibitors inhibited the production of IL-6 and IL-8 stimulated by IL-1β+Aβ (25–35) (Fig. 4A).

Based on the results showing the inhibitory effect of MAPK inhibitors on IL-1β+Aβ (25–35)-induced cytokine production, we investigated whether EGCG could suppress activation of p38 and JNK in human astrocytoma, U373MG cells. First, the time course of IL-1β+Aβ (25–35)-induced p38 MAPK and JNK phosphorylation is shown in Fig. 4B. We showed that phosphorylation of p38 MAPK and JNK was transient and peaked at 1 to 2 h, after stimulation with IL-1β+Aβ (25–35) in human astrocytoma, U373MG cells.

Next, to investigate whether EGCG has influence on the phosphorylation of p38 MAPK and JNK-induced by IL-1β+Aβ (25–35) for 1 h, we pretreated EGCG (2–20 μM) before stimulation with IL-1β+Aβ (25–35). The results showed that EGCG reduced the phosphorylation of p38 MAPK and JNK in IL-1β+Aβ (25–35)-stimulated human astrocytoma, U373MG cells (Fig. 4C).

3.5. Effect of EGCG on MKP-1 induction

To determine whether EGCG can modulate MKP-1 expression, RT-PCR and Western blot analysis were

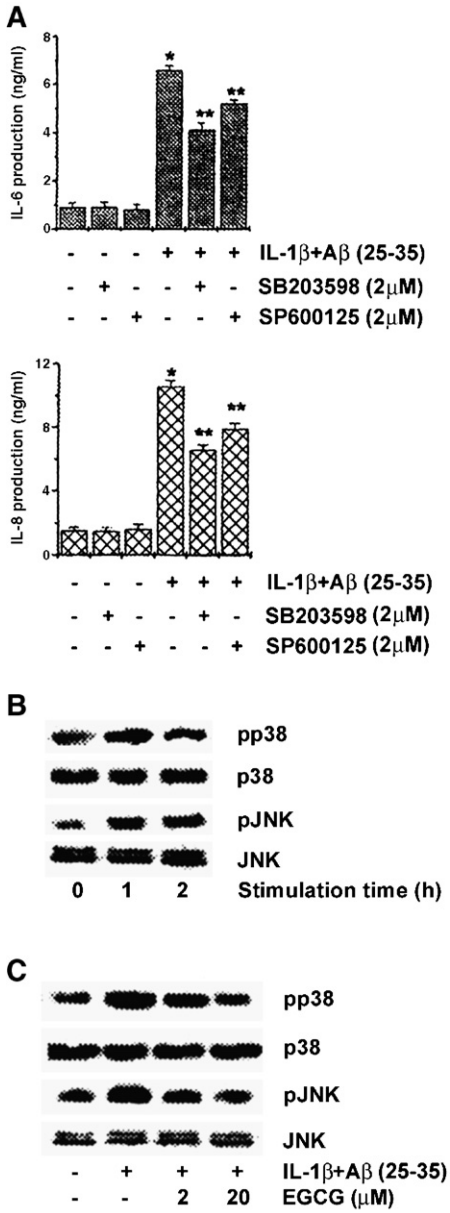

Fig. 4. Effect of EGCG on MAPK pathway. (A) Cells (3×10^5 cells/ml) were pretreated with MAPK inhibitor, SB203580 (2 μM) and SP600125 (5 μM) for 1 h before stimulation of IL-1β (10 ng/ml) plus Aβ (25–35) (30 μM) for 24 h. The amount of IL-6 and IL-8 production was measured using the ELISA method. (B) 5×10^6 cells were treated with IL-1β plus Aβ (25–35) from 1 to 2 h, and then the phosphorylation of p38 MAPK and JNK was determined by Western blot analysis as described in Materials and Methods using specific anti-phospho-MAPKs Abs and anti-total MAPKs Abs. (C) 5×10^6 cells were preincubated for 2 h with 2 or 20 μM EGCG and then treated with IL-1β (10 ng/ml) plus Aβ (25–35) (30 μM) for 1 h, and then the phosphorylation of p38 MAPK and JNK was determined by Western blot analysis using specific anti-phospho-MAPKs. Data represent the mean±S.E.M. of three independent experiments. *$P<.05$, significantly different from the unstimulated cells. **$P<.05$, significantly different from the IL-1β plus Aβ-stimulated cells.

performed. As shown in Fig. 5A, pretreatment of EGCG (20 μM) induced MKP-1 mRNA expression. We also showed that pretreatment of EGCG induced MKP-1 protein expression (Fig. 5B). To confirm these results, expression of MKP-1 in human astrocytoma, U373MG cells, was visualized using confocal microscopy. After 2 h of treatment with 20 μM EGCG, staining for the MKP-1 protein indicated that EGCG induced MKP-1 expression (Fig. 5C).

In order to demonstrate the involvement of MKP-1 concretely, we used Ca^{2+}-channel blockers. To block the MKP-1 activation, we used flunarizine (T-type Ca^{2+}-channel blocker) and nifedipine (L-type Ca^{2+}-channel blocker). As shown in Fig. 5D, IL-1β+Aβ (25–35) caused a significant increase in IL-6, IL-8 and VEGF production, and flunarizine (10 μM) and nifedipine (100 nM) significantly augmented these increases. In addition, we showed that EGCG inhibited the cytokine levels enhanced by Ca^{2+}-channel blocker (Fig. 5E).

4. Discussion

Green tea polyphenols, which comprise 30% of the dry weight of green tea leaves, include EGCG, epigallocatechin, epicatechin-3-gallate and epicatechin. EGCG is the most abundant of these catechins and it has been attributed with many healthful benefits. Other study reported that EGCG prevents Aβ-induced hippocampal neuronal cell death through its antioxidant property [28]. Therefore, daily intakes of green tea may reduce the risk of AD by helping get rid of reactive oxygen species induced by Aβ. Also, the anti-inflammatory action of EGCG has been studied by many groups and in many cell types and is considered to be a strong anti-inflammatory agent. Although activation of microglia and astrocytes is a major cause in AD, there is no report that EGCG regulates the secretion of cytokine from astrocyte stimulated by pathology production of AD. In this study, we investigated the regulatory effect of EGCG in IL-1β+Aβ-stimulated human astrocytoma cells.

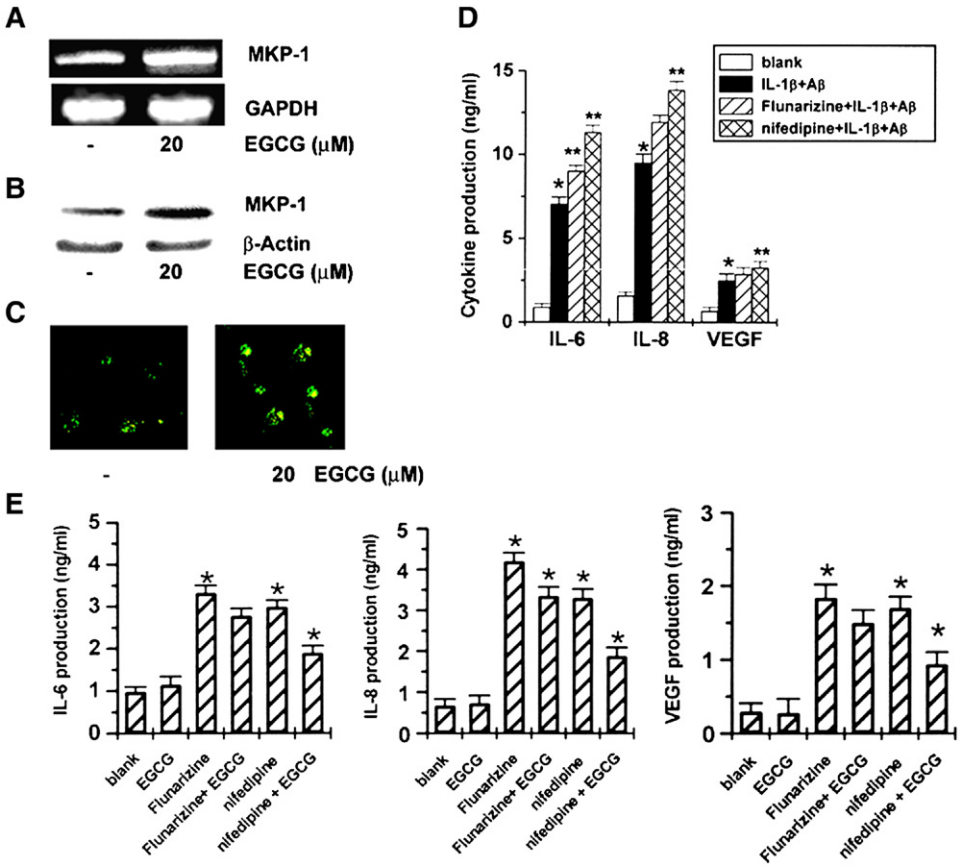

Fig. 5. Effect of EGCG on MKP-1 expression. (A) 5×10^6 cells were treated with 20 μM EGCG for 1 h and then the expression of MKP-1 mRNA was determined by RT-PCR. (B) 5×10^6 cells were treated with 20 μM EGCG for 2 h and then the expression of MKP-1 was determined by Western blot analysis. (C) 3×10^5 cells were preincubated for 2 h with EGCG (20 μM). Cells were fixed with 4% paraformaldehyde in PBS, permeabilized with 0.2% Triton X-100 in PBS and blocked with 1.5% BSA. Polyclonal antibodies to MKP-1 were applied for 1 h. After washing, the cells were incubated with fluorescein isothiocyanate-conjugated donkey anti-rabbit IgG and then analysed using a confocal microscope. (D) Cells (3×10^5 cells/ml) were pretreated with flunarizine (10 μM) and nifedipine (100 nM) for 1 h before stimulation of IL-1β (10 ng/ml) plus Aβ (25–35) (30 μM) for 24 h. (E) Cells (3×10^5 cells/ml) were pretreated with flunarizine (10 μM) and nifedipine (100 nM) and then treated with EGCG (20 μM). The amount of IL-6, IL-8 and VEGF production was measured using the ELISA method. *$P<.05$, significantly different from the unstimulated cells. **$P<.05$, significantly different from the IL-1β plus Aβ-stimulated cells.

AD is the most common cause of dementia, and its pathological changes include Aβ deposits, neurofibrillary tangles and a variety of "inflammatory" phenomenon such as activation of microglia and astrocytes [29]. Aβ peptide induces pro-inflammatory cytokine and chemokine secretion in rat astrocytes and human astrocytoma cells. IL-1β is a critical inflammatory cytokine in AD, and IL-1β and Aβ are responsible for microglia stimulation [30] and induce inflammatory response. Inflammatory cytokines are important pathologic factors of progression of AD, neuropathologic changes and inflammation in the CNS [31]. In the brain of AD patients, the high expression of VEGF in neuronal as well as glial cells was observed since cerebrovascular pathologies associated with AD cause cerebral ischemia. In the present study, we showed that the pretreatment of EGCG not only inhibited the expression of IL-6, IL-8 and VEGF but also had no toxic effects in human astrocytoma cells. Therefore, these results suggested that EGCG has an anti-inflammatory effect through regulation of inflammatory cytokine expression in astrocytoma cells.

Many studies reported that EGCG-mediated regulation of the inflammatory pathway might be cell-type specific. In macrophage cell line, EGCG alone up-regulates COX-2 expression and PGE_2 production [24,32], whereas EGCG significantly inhibited COX-2 expression in colon cancer cell lines [33]. These results suggest that EGCG regulates COX-2-mediated inflammation through different mechanisms in different cell systems. We observed the PGE_2 production, and COX-2 expression level induced by IL-1β+Aβ [25–35] was inhibited by EGCG in human astrocytoma cells. In contrast to our results, a report by Kim et al. [34] demonstrated that EGCG induced COX-2 expression and PGE_2 synthesis through PKC and p38. We postulated that apoptosis signal might be involved at high concentration of EGCG. Therefore, the concentration that did not affect cell viability and morphology was chosen in this study. This suggests that EGCG at lower concentration may affect the anti-inflammatory pathway and may have a beneficial effect in the treatment of COX-2-mediated AD.

NF-κB plays a critical role in the expression of many genes involved in immune and inflammatory responses [35,36]. Other research reported that chronic administration of indomethacin by blocking the activation of the NF-κB is significantly reduced in AD in vivo model and provided insights into the mechanisms by which this drug could slow the progression of AD [37]. We postulated that EGCG mediates its effects at least partly through suppression of NF-κB activation. In this study, we showed that pretreatment of EGCG (20 μM) inhibited the IL-1β+Aβ (25–35)-stimulated increase of the nuclear RelA/p65 levels and NF-κB binding activity in U373MG. In addition, EGCG (20 μM) significantly inhibited IL-1β+Aβ (25–35)-induced IκB-α degradation. These results demonstrated that the anti-inflammatory properties of EGCG are mediated by down-regulating NF-κB activation in U373MG cells (Fig. 6).

MAPKs (p38 MAPK, ERK and JNK) have been demonstrated in AD progression. Activation of MAPKs located in microglial cells could represent the initial step in a feed-forward inflammatory process, resulting in the production of cytokines and activation of other inflammatory mediators, such as iNOS and COX-2 [38,39]. In the present study, we showed that MAPK inhibitors suppressed cytokine (IL-6 and IL-8) production induced by IL-1β+Aβ (25–35). These results suggested that MAPK signaling pathways are involved in an inflammatory response induced by IL-1β+Aβ (25–35) in U373MG cells. Previously, other

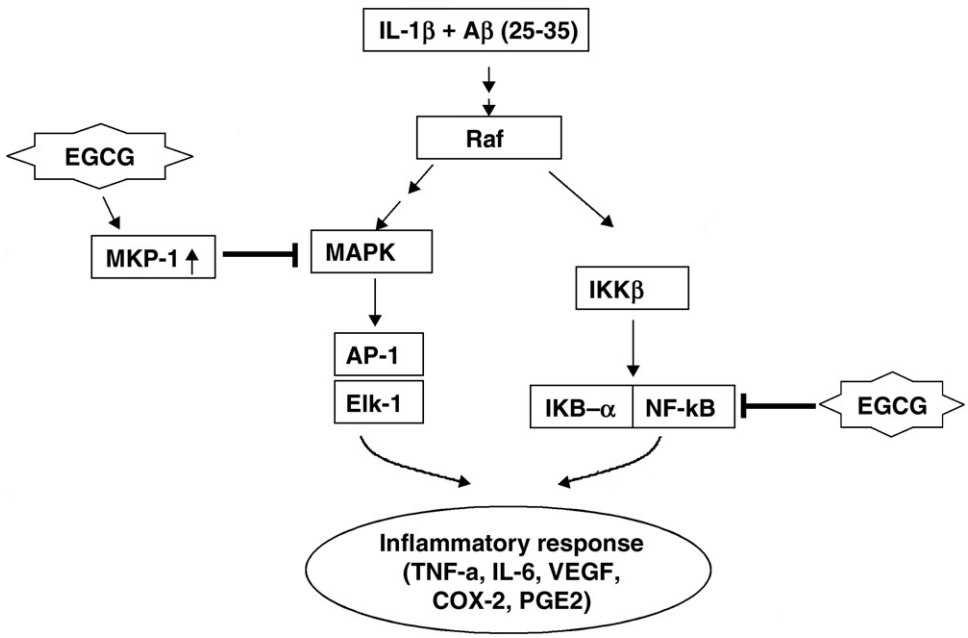

Fig. 6. Proposed mechanism of EGCG-mediated anti-inflammatory effect in IL-1β plus Aβ (25–35)-stimulated U373MG cells.

studies demonstrated that the p38MAPK pathway, a major proinflammatory signal transduction mechanism, is hyperactivated in the AD brain. In addition, we observed that EGCG inhibited the activation of ERK (data not shown). Yoshino et al. [27] reported that enhancement of cytokine occurs through induction and activation of p38 and/or JNK pathway in human astrocytoma cells. Also, they showed that inhibitors of ERK and PI3 did not regulate cytokine production. For these reasons, we investigated the effect of EGCG on activation of p38 and JNK. In this study, we confirmed that pretreatment of EGCG (2–20 μM) suppressed the activation of p38 MAPK and JNK induced by IL-1β+Aβ (25–35).

MKP-1 is a critical negative regulator in response to inflammatory stimuli and is responsible for switching off the production of proinflammatory cytokines. Previously, MKP-1 is induced by certain anti-inflammatory drugs/agents and it was proposed that MKP-1 could be a target for developing novel anti-inflammatory drugs [40]. MKP-1 was induced concurrently with the inactivation of p38, ERK and JNK, whereas blocking MKP-1 induction prevented this inactivation. Overexpression of MKP-1 accelerated JNK and p38 inactivation and substantially inhibited the production of TNF-α and IL-6 [41]. Other studies reported that the immunosuppressant FK506 (Tacrolimus) induces MKP-1 expression [42] and provides a novel strategy to enhance survival and functional recovery of damaged neurons in the adult mammalian brain. In the present study, we showed that EGCG induced MKP-1 expression. From this, we speculate that IL-1β+Aβ (25–35) would not activate MAPK because MKP-1 was induced by pretreatment of EGCG in advance. In addition, we used Ca^{2+}-channel blockers to block MKP-1 activation. We showed that suppression of MKP-1 induced cytokine production, and EGCG inhibited the cytokine production induced by Ca^{2+}-channel blockers. Therefore, we project that the anti-inflammatory effect of EGCG, at least in part, might occur through induction of MKP-1 regulation and cytokine production (Fig. 6). However, further study is necessary to explain the precise role of EGCG in relation between MKP-1 induction and the MAPK pathway in U373MG cells.

Several animal studies have shown that peripheral administration of EGCG (50 mg/kg ip) exerted neuroprotective effects in two gerbil models of ischemia, inhibiting the increase of polyamine and malondialdehyde levels in the cerebral cortex and hippocampus [43,44]. [^{3}H]-EGCG has been found in the brain 24 h after an intraperitoneal injection [45], suggesting that EGCG does in fact cross the blood–brain barrier, which may account for its neurological/neuroprotective activities. These data suggest that a regular consumption of green tea may enable the brain to maintain a fairly high level of EGCG [46]. Also, several studies in AD animal models suggest that EGCG from green tea may affect several potential targets associated with AD progression [47,48]. Rezai-Zadeh et al. [48] reported that EGCG was administered intraperitoneally to Alzheimer Swedish mutant APP overexpressing mice (Tg APPsw mice) and found a significant reduction in cerebral Aβ levels concomitant with reduced β-amyloid plaques. These suggest that EGCG administration to AD patients might be an effective prophylactic strategy for reduction of cerebral amyloidosis. Although EGCG attenuated COX-2 expression and MAPK activation in vitro, the effect of EGCG on an in vivo model of AD is not elucidated in the present study. Thus, further investigation with an in vivo model is under consideration.

In conclusion, we have shown that EGCG can regulate the inflammatory response induced by IL-1β+Aβ (25–35) in U373MG cells. EGCG affects the expression of inflammatory genes through regulation of the NF-κB/IκB-α pathway. In addition, EGCG suppressed MAPK activation and induced MKP-1 expression. Induced MKP-1 would modulate MAPK activation, and thus inflammatory genes might be inhibited. The data presented in this study could help in elucidating the epidemiological findings indicating that EGCG reduces the risk of developing AD and may slow its progression.

Acknowledgments

This study was supported by the SRC program of KOSEF (R11-2005-014), and by a grant (A050376) from the Korea Health 21 R&D Project, Ministry of Health and Welfare, Republic of Korea.

References

[1] Parihar MS, Hemnani T. Alzheimer's disease pathogenesis and therapeutic interventions. J Clin Neurosci 2004;11:456–67.
[2] Ferencik M, Novak M, Rovensky J, Rybar I. Alzheimer's disease inflammation and non-steroidal anti-inflammatory drugs. Bratisl Lek Listy 2001;102:123–32.
[3] Iversen LL, Mortishire-Smith RJ, Pollack SJ, Shearman MS. The toxicity in vitro of beta-amyloid protein. Biochem J 1995;311:1–16.
[4] Forloni G, Mangiarotti F, Angeretti N, Lucca E, De Simoni MG. Beta-amyloid fragment potentiates IL-6 and TNF-alpha secretion by LPS in astrocytes but not in microglia. Cytokine 1997;9:759–62.
[5] Gitter BD, Cox LM, Rydel RE, May PC. Amyloid beta peptide potentiates cytokine secretion by interleukin-1 beta-activated human astrocytoma cells. Proc Natl Acad Sci U S A 1995;92:10738–41.
[6] Gruol DL, Nelson TE. Physiological and pathological roles of interleukin-6 in the central nervous system. Mol Neurobiol 1997;15:307–39.
[7] Ferrara N. Role of vascular endothelial growth factor in regulation of physiological angiogenesis. Am J Physiol Cell Physiol 2001;280(6):1358–66.
[8] Thomas KA. Vascular endothelial growth factor, a potent and selective angiogenic factor. J Biol Chem 1996;271(2):603–6.
[9] Yancopoulos GD, Davis S, Gale NW, Rudge JS, Wiegand SJ, Holash J. Vascular-specific growth factors and blood vessel formation. Nature 2000;407:242–8.
[10] Marti HH, Risau W. Systemic hypoxia changes the organ-specific distribution of vascular endothelial growth factor and its receptors. Proc Natl Acad Sci U S A 1998;95:15809–14.
[11] Marti HJ, Bernaudin M, Bellail A, Schoch H, Euler M, Petit W. Hypoxia-induced vascular endothelial growth factor expression

precedes neovascularization after cerebral ischemia. Am J Pathol 2000;156:965–76.
[12] Rohrenbeck AM, Bette M, Hooper DC, Nyberg F, Eiden LE, Dietzschold B, et al. Upregulation of COX-2 and CGRP expression in resident cells of the Borna disease virus-infected brain is dependent upon inflammation. Neurobiol Dis 1999;6:15–34.
[13] Chang L, Karin M. Mammalian MAP kinase signalling cascades. Nature 2001;410:37–40.
[14] Morishima Y, Gotoh Y, Zieg J, Barrett T, Takano H, Flavell R, et al. Beta-amyloid induces neuronal apoptosis via a mechanism that involves the c-Jun N-terminal kinase pathway and the induction of Fas ligand. J Neurosci 2001;21:7551–60.
[15] Hensley K, Floyd RA, Zheng NY, Nael R, Robinson KA, Nguyen X, et al. p38 kinase in activated in the Alzheimer's disease brain. J Neurochem 1999;72:2053–8.
[16] Zhu X, Rottkamp CA, Hartzler A, Sun Z, Takeda A, Boux H, et al. Activation of MKK6, an upstream activator of p38, in Alzheimer's disease. J Neurochem 2001;79:311–8.
[17] Sakaue H, Ogawa W, Nakamura T, Mori T, Nakamura K, Kasuga M. Role of MAPK phosphatase-1 (MKP-1) in adipocyte differentiation. J Biol Chem 2004;279:39951–7.
[18] Wadgaonkar R, Pierce JW, Somnay K, Damico RL, Crow MT, Collins T, et al. Regulation of c-Jun N-terminal kinase and p38 kinase pathways in endothelial cells. Am J Respir Cell Mol Biol 2004; 31:423–31.
[19] Dufresne CJ, Farnworth ER. A review of latest research findings on the health promotion properties of tea. J Nutr Biochem 2001; 12:404–21.
[20] Yang CS, Chung JY, Yang G, Chhabra SK, Lee MJ. Tea and tea polyphenols in cancer prevention. J Nutr 2000;130:472S–8S.
[21] Stoner GD, Mukhtar H. Polyphenols as cancer chemopreventive agents. J Cell Biochem 1995;22:169–80.
[22] Aktas O, Prozorovski T, Smorodchenko A, Savaskan NE, Lauster R, Kloetzel PM, et al. Green tea epigallocatechin-3-gallate mediates T cellular NF-kappa B inhibition and exerts neuroprotection in autoimmune encephalomyelitis. J Immunol 2004;173: 5794–800.
[23] Haqqi TM, Anthony DD, Gupta S, Ahmad N, Lee MS, Kumar GK, et al. Prevention of collagen-induced arthritis in mice by a polyphenolic fraction from green tea. Proc Natl Acad Sci U S A 1999; 96:4524–9.
[24] Park JW, Choi YJ, Suh SI, Kwon TK. Involvement of ERK and protein tyrosine phosphatase signaling pathways in EGCG-induced cyclooxygenase-2 expression in raw 264.7 cells. Biochem Biophys Res Commun 2001;286:721–5.
[25] Jeong HJ, Na HJ, Hong SH, Kim HM. Inhibition of the stem cell factor-induced migration of mast cells by dexamethasone. Endocrinology 2003;144:4080–6.
[26] Schoonbroodt S, Legrand-Poels S, Best-Belpomme M, Piette J. Activation of the NF-B transcription factor in a T-lymphocytic cell line by hypochlorous acid. Biochem J 1997;321:777–85.
[27] Yoshino Y, Aoyagi M, Tamaki M, Duan L, Morimoto T, Ohno K. Activation of p38 MAPK and/or JNK contributes to increased levels of VEGF secretion in human malignant glioma cells. Int J Oncol 2006;29(4):981–7.
[28] Choi YT, Jung CH, Lee SR, Bae JH, Baek WK, Suh MH, et al. The green tea polyphenol (−)-epigallocatechin gallate attenuates beta-amyloid-induced neurotoxicity in cultured hippocampal neurons. Life Sci 2001;70:603–14.
[29] Meda L, Bonaiuto C, Szendrei GI, Ceska M, Rossi F, Cassatella MA. Beta-amyloid (25–35) induces the production of interleukin-8 from human monocytes. J Neuroimmunol 1995;59:29–34.
[30] Akama KT, Van Eldik LJ. Beta-amyloid stimulation of inducible nitric-oxide synthase in astrocytes is interleukin-1beta- and tumor necrosis factor-alpha (TNFalpha)-dependent, and involves a TNFalpha receptor-associated factor- and NFkappaB-inducing kinase-dependent signaling mechanism. J Biochem 2000;275:7918–24.
[31] Raivich G, Bohatschek M, Kloss CUA, Werner A, Jones LL, Kreutzberg GW. Neuroglial activation repertoire in the injured brain: graded response, molecular mechanisms and cues to physiological function. Brain Res Rev 1999;30:77–105.
[32] Butterfield DA. Amyloid beta-peptide [1–42]-associated free radical-induced oxidative stress and neurodegeneration in Alzheimer's disease brain: mechanisms and consequences. Curr Med Chem 2003;10:2651–9.
[33] Peng G, Dixon DA, Muga SJ, Smith TJ, Wargovich MJ. Green tea polyphenol (−)-epigallocatechin-3-gallate inhibits cyclooxygenase-2 expression in colon carcinogenesis. Mol Carcinog 2006;45(5): 309–19.
[34] Kim SY, Ahn BH, Min KJ, Lee YH, Joe EH, Min do S. Phospholipase D isozymes mediate epigallocatechin gallate-induced cyclooxygenase-2 expression in astrocyte cells. J Biol Chem 2004;279(37):38125–33.
[35] Tegeder I, Pfeilschifter J, Geisslinger G. Cyclooxygenase-independent actions of cyclooxygenase inhibitors. FASEB J 2001;15:2057–72.
[36] Ghosh S, May MJ, Kopp EB. NF-kB and Rel proteins: evolutionarily conserved mediators of immune responses. Annu Rev Immunol 1998; 16:225–60.
[37] Sung S, Yang H, Uryu K, Lee EB, Zhao L, Shineman D, et al. Modulation of nuclear factor-kappa B activity by indomethacin influences A beta levels but not A beta precursor protein metabolism in a model of Alzheimer's disease. Am J Pathol 2004;165:2197–206.
[38] Hoozemans JJ, Veerhuis R, Rozemuller AJ, Arendt T, Eikelenboom P. Neuronal COX-2 expression and phosphorylation of pRb precede p38 MAPK activation and neurofibrillary changes in AD temporal cortex. Neurobiol Dis 2004;15:492–9.
[39] Ayasolla K, Khan M, Singh AK, Singh I. Inflammatory mediator and beta-amyloid (25–35)-induced ceramide generation and iNOS expression are inhibited by vitamin E. Free Radic Biol Med 2004; 37:325–38.
[40] Lasa M, Abraham SM, Boucheron C, Saklatvala J, Clark AR. Dexamethasone causes sustained expression of mitogen-activated protein kinase (MAPK) phosphatase 1 and phophatase-mediated inhibition of MAPK p38. Mol Cell Biol 2002;22:7802–11.
[41] Chen P, Li J, Barnes J, Kokkonen GC, Lee JC, Liu Y. Restraint of proinflammatory cytokine biosynthesis by mitogen-activated protein kinase phosphatase-1 in lipopolysaccharide-stimulated macrophages. J Immunol 2002;169:6408–16.
[42] Winter C, Schenkel J, Zimmermann M, Herdegen T. MAP kinase phosphatase 1 is expressed and enhanced by FK506 in surviving mamillary, but not degenerating nigral neurons following axotomy. Brain Res 1998;801:198–205.
[43] Lee SY, Kim CY, Lee JJ, Jung JG, Lee SR. Effects of delayed administration of (−)-epigallocatechin gallate, a green tea polyphenol on the changes in polyamine levels and neuronal damage after transient forebrain ischemia in gerbils. Brain Res Bull 2003;61: 399–406.
[44] Lee S, Suh S, Kim S. Protective effects of the green tea polyphenol (-)-epigallocatechin gallate against hippocampal neuronal damage after transient global ischemia in gerbils. Neurosci Lett 2000; 287:191–4.
[45] Nagai K, Jiang MH, Hada J, Nagata T, Yajima Y, Yamamoto S, et al. (-)-Epigallocatechin gallate protects against NO stress induced neuronal damage after ischemia by acting as an anti-oxidant. Brain Res 2002;956:319–22.
[46] Suganuma M, Okabe S, Oniyama M, Tada Y, Ito H, Fujiki H. Wide distribution of [^{3}H] (-)-epigallocatechin gallate, a cancer preventive tea polyphenol, in mouse tissue. Carcinogenesis 1998;19:1771–6.
[47] Jeon SY, Bae K, Seong YH, Song KS. Green tea catechins as a BACE1 (beta-secretase) inhibitor. Bioorg Med Chem Lett 2003;13: 3905–8.
[48] Rezai-Zadeh K, Shytle D, Sun N, Mori T, Hou H, Jeanniton D, et al. Green tea epigallocatechin-3-gallate (EGCG) modulates amyloid precursor protein cleavage and reduces cerebral amyloidosis in Alzheimer transgenic mice. J Neurosci 2005;25:8807–14.